

# DESIGN AND FINITE ELEMENT ANALYSIS OF AN EXTRACTOR MACHINE FOR CASTOR OIL BIODIESEL PRODUCTION

Linus Adache Adache <sup>a</sup>, Taye Stephen Mogaji <sup>b1</sup>, Mohammed Olabanji Olayinka <sup>b2,c</sup>,  
Zephaniah Ayodeji Olagoke <sup>b3</sup>

<sup>a</sup>Air Force Institute of Technology (AFIT), Kaduna, Nigeria.

<sup>b</sup>Federal University of Technology, Akure, Ondo State, Nigeria.

<sup>c</sup>School of Engineering and Engineering Technology, PMB 704, Ondo State, Nigeria.

<sup>a</sup>[linusadache@gmail.com](mailto:linusadache@gmail.com), <sup>b1</sup>[mogajits@gmail.com](mailto:mogajits@gmail.com), <sup>b2</sup>[obayinclox@gmail.com](mailto:obayinclox@gmail.com), <sup>b3</sup>[gokeayodeji@gmail.com](mailto:gokeayodeji@gmail.com)

## Abstract:

This research presents the design of a castor oil extractor for producing castor oil biodiesel. The machine was designed using appropriate design equations in the design analysis of the machine, and finite element analysis was conducted to determine the structural integrity, functionality and manufacturability of the system. With a total load distribution of 729 kN resulting from the screw shaft and the weight of other accessories, the behaviour of the frame material under different loading conditions was stated. Solidworks/Ansys analysis of the screw shaft showed a maximum stress distribution of  $5.26 \times 10^{-4}$  MPa, which is below the yield strength of 460 MPa for the material used. The maximum deformation under loading conditions is  $4.24 \times 10^{-4}$  mm, which is negligible and does not pose a risk of failure of the machine. The fabrication was done using locally available materials. The performance of the developed machine was evaluated using castor seed and obtained output capacity of 120.2 kg/h and extraction efficiency of 58% respectively at a speed of 30 rpm. The machine can function independently for extracting castor oil and can also be used to extract oil from other seeds of similar sizes as castor seed, thereby minimizing challenges associated with conventional extracting machines.

**Keywords:** extractor machine; castor oil; biodiesel production; finite element analysis; renewable energy.

**Cite as:** Adache Adache, L., Mogaji, T.S., Olabanji Olayinka, M., Ayodeji Olagoke, Z. (2025). Design and finite element analysis of an extractor machine for castor oil biodiesel production. *J Appl Res Eng Technol & Engineering*, 6(1), 21917. <https://doi.org/10.4995/jarte.2025.21917>

## 1. Introduction

In many parts of the world, virgin vegetable oils serve as the primary source of biodiesel oil feedstock. This includes oils from nuts, seeds, and beans, such as rapeseed or soybean oil, as well as oil derived from palm and various other vegetable sources. The seeds need to be crushed into a powder form or paste for oil extraction and biodiesel oil production. Crushing involves squeezing the oil seeds feedstock into fine particles or paste, accomplished by rotating parts against a fixed part through applied force, impact, and shearing. When the strain in the feedstock exceeds its elastic limit due to applied pressure, impact forces, or shearing effects, pulverization occurs (Ejiroghene, 2021; Zulqarnain et al., 2021). The main components of the extracting machine are a frame, feeding hopper, extrusion screw, heating element cover, bearings, base hopper, and an electric motor. Mechanical oil extraction is the most conventional method for large-scale oil extraction (Ojo et al., 2022; Linus et al., 2023). This can be achieved using a manual press or an automatic screw press oil expeller; however, these methods have drawback as it has a relatively inadequate oil yield (Sarip et al., 2016; Muhammad & Sohail, 2024). Over the years, several researchers have worked in this area, according to Omojola & Daramy

(2023) investigated the application of machine learning technologies in biodiesel production process. The outcome of this current study will help to stimulate further investigation on the application of novel and innovative technologies that can enhance biodiesel production. In another study, Naquib & Faisal (2020) utilized the Taguchi design methodology and design experiments to develop and evaluate the performance of an optimized screw-type domestic oil expeller. The authors found that locally available oil expeller machines were associated with low oil extraction output, high power consumption, and lack of compactness due to their large weight. The research resulted in an enhanced screw-type oil expeller machine designed for local use to meet consumer demands. Considering the established environmental impact of fossil fuel consumption and the need for alternative energy production, societies worldwide are experiencing a significant and urgent need for changes in energy production and consumption, which is one of the major focuses of this study (Ziemiński & Fraç, 2012). Furthermore, Chibuye et al. (2023) reported that extraction techniques offer significant advantages over conventional methods. Traditional extraction techniques are characterized by longer extraction times, higher solvent requirements, a risk of losing bioactivity, and lower yields. In contrast, modern techniques provide many benefits, such as

\*Corresponding author: M. Ruiz, [maria Ruiz@gmail.com](mailto:maria Ruiz@gmail.com)

reduced extraction time, lower solvent demands, better preservation of biological activities, higher yields, and decreased energy requirements. Related studies show that biofuel production and utilization offer sustainable solutions for enhancing local and national energy security, economic growth, rural economic diversification, employment and import substitution (Teklit et al., 2021; Vikram et al., 2024; Fatima et al., 2022). These benefits have direct and indirect impacts on trade balance, energy supply diversification, and the establishment of new industries (Teklit et al., 2021; Vikram et al., 2024; Fatima et al., 2022).

The novelty in our research lies in the integration of a heater or heating element in the extracting chamber of the automatic machine to reduce viscosity in the paste, thereby increasing oil production yield, reducing time consumption, and simplifying the oil production process. As pointed out by Wunuken et al. (2019); Rattanaphra & Srinophakun (2010) the obtained oil can be transesterified to produce biodiesel. Biodiesel as an alternative fuel has garnered attention globally due to its renewable, biodegradable, and environmentally friendly nature. Findings from previous studies of (Ragul et al., 2019; Said et al., 2024; Wadhah et al., 2022) have shown that biodiesel produces lower pollutant emissions, has a high flash point, offers improved lubrication qualities, and has a high cetane number, with physical and chemical properties similar to petroleum diesel.

With the view of developing efficient automatic oil extractor that will aid production and make alternative energy (fuel) available in fulfilling net zero emission, an improved design and finite element analysis of an extractor machine for castor oil biodiesel production is carried out in this research. Castor seeds were chosen as the feedstock for oil extraction for biodiesel production due to their interesting properties, such as very low cloud and pour points, making them suitable for use in extreme cold weather conditions (Jour et al., 2004; Sánchez et al., 2015; Adewale et al., 2016; Fadhil et al., 2016; Krishna et al., 2016; Sujata et al., 2022).

The literature review suggests that incorporating a heating element in the extraction chamber of oil extractor machines could improve efficiency and increase oil yield. In this research, a castor oil extraction machine was designed using SolidWorks software, and finite element analysis was conducted to assess the structural integrity, functionality, and manufacturability of the system. This machine was subsequently used to produce castor oil biodiesel.

## 2. Materials and Methods

SolidWorks 2022 and Ansys 2021 software were used for designing the castor oil extractor and its components. Finite element analysis was also conducted to determine the structural integrity and manufacturability of the machine. Locally available materials, specifically mild steel obtained from Partaker in Kaduna, Nigeria, were used for fabricating the extractor machine. Mild steel was selected for key components due to the following reasons:

- i Strength: Mild steel can withstand significantly greater tension before failure compared to materials like aluminum. The tensile strength of mild steel typically ranges from 400 MPa to 500 MPa, while aluminum is around 90 MPa (Maigul et al., 2023).
- ii Cost: Mild steel is the least expensive among various types of steel, including stainless steel and aluminum, due to its carbon content, which provides sufficient strength at an affordable price (Kyaw et al., 2019).
- iii Durability: Mild steel is known for its durability, making it ideal for this research.
- iv Machinability: Its low carbon content makes mild steel easier to machine and weld. This machinability is advantageous for general fabrication, leading to its selection over stainless steel and aluminum (Moses, 2016; Habib et al., 2016).
- v Corrosion resistance: Although mild steel is prone to oxidation and rust, these drawbacks can be mitigated by applying a protective coating to prevent corrosion (Rufus et al., 2015; Ketan et al., 2017).
- vi Thermal conductivity: Mild steel conducts both electricity and heat effectively, though aluminum dissipates heat about 15 times faster (Yunus & Afshin., 2015).

### 2.1. Design consideration

Factors considered in the design of the castor oil extractor include:

- i Maximum oil extraction output
- ii Minimal oil extraction loss
- iii Improved oil quality
- iv Easy assembly
- v Availability of fabrication materials
- vi Ensuring extreme pressing of worm shaft.

### 2.2. Material selection criteria

Some design criteria considered in the selection of materials for fabricating the castor oil extractor, aimed at enhancing its efficiency, reliability, manufacturability, stability and sustainability, include:

- i. Corrosion resistance: Careful consideration is given to selecting materials for each component of the extractor to prevent corrosion and oil contamination.
- ii. Material flow and ergonomics: The flow of material is important in process flow design. Consideration was given to the ease of operating the machine effectively and efficiently to optimize human well-being and overall castor oil extractor machine performance.
- iii. Manufacturability: This refers to the ease with which the design can be executed and the castor oil extractor machine to be fabricated.

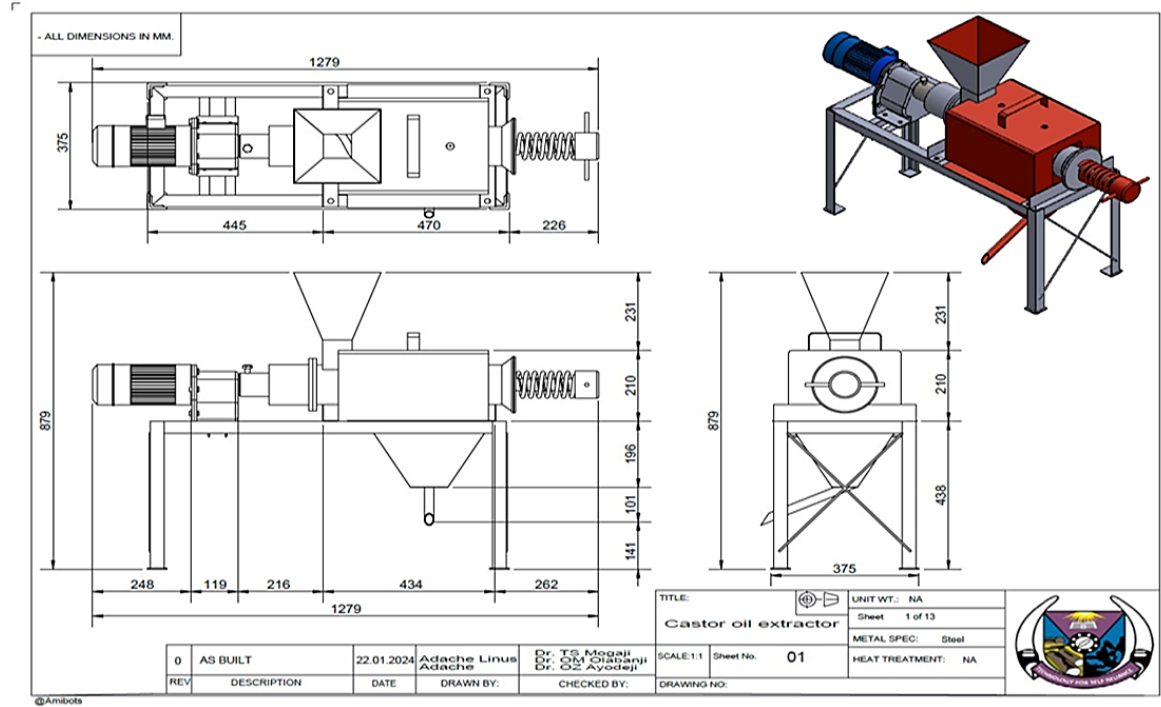


Figure 1: Orthographic projection of extractor.

### 2.3. Design drawings of the castor oil extractor

The detailed design drawings of the castor oil extractor were completed using SOLIDWORKS software 2022. Design analysis and calculations for various components of the machine were conducted using appropriate design equations. To ensure that no part of the machine fails during fabrication, section-by-section simulation of individual machine parts was carried out using ANSYS

software 2021. The main components of castor oil extractor include the frame, extrusion screw, feeding hopper, base hopper, heating element cover and an electric motor. The isometric view of the extractor and orthographic views showing the front, side, and plan views are presented in Figure 1, with the exploded view shown in Figure 2.

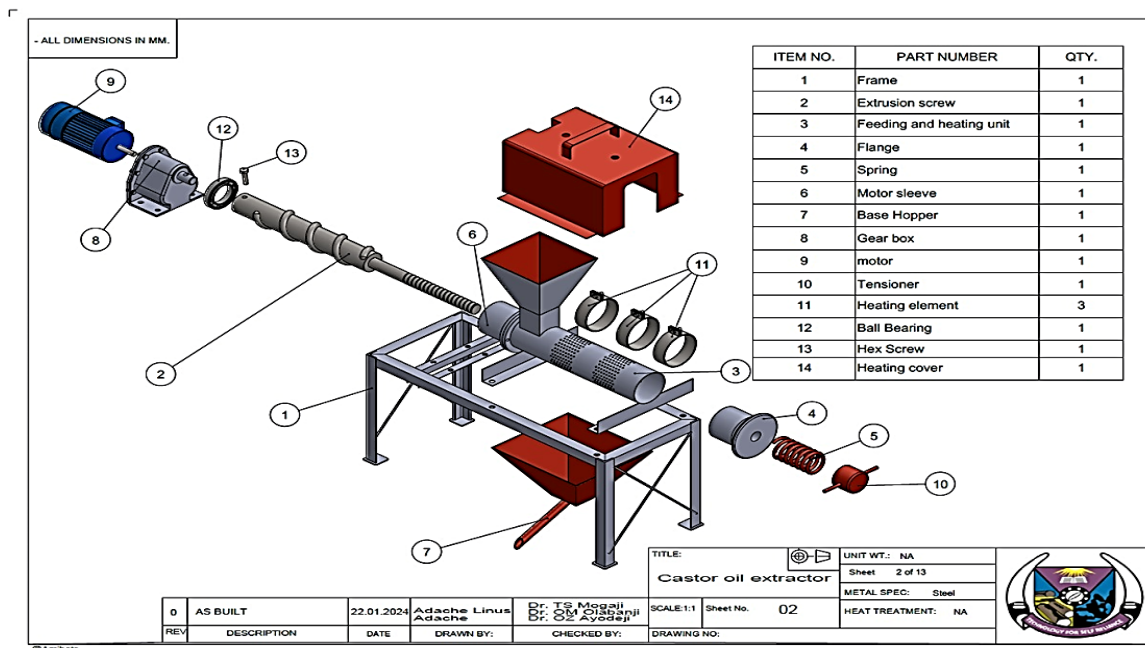


Figure 2: Exploded view of the extractor.

## 2.4. Design analysis for castor oil extractor

### 2.4.1. Determination of volume of a hopper

The volume of hopper (V<sub>H</sub>) is projected from the similarity of a square frustum with a base attachment as shown in Figure 3. The volume of frustum is determined using the relation for the volume of a pyramid given in Equation 1. Hence, Equations (1-12) was obtained from (Salawu et al., 2015; Ali & Watson, 2014; Kuku et al., 2020; Oji et al., 2019; Yakubu et al., 2020; Azeez et al., 2019).

$$\text{Volume of pyramid} = \frac{1}{3} AH \quad (1)$$

Where;

A is the area of base and H is the height of the pyramid.

Volume of frustum

$$ABCDabcd = \frac{1}{3} (AH - ah) \quad (2)$$

Where;

$\frac{1}{3} AH$  and  $\frac{1}{3} ah$  is the volume of pyramids ABCD and abcd respectively.

$$\text{Hence, Volume of hopper, } V_H = V_F + V_A \quad (3)$$

Where;

V<sub>F</sub> is the volume of frustum

V<sub>A</sub> is the Volume base attachment

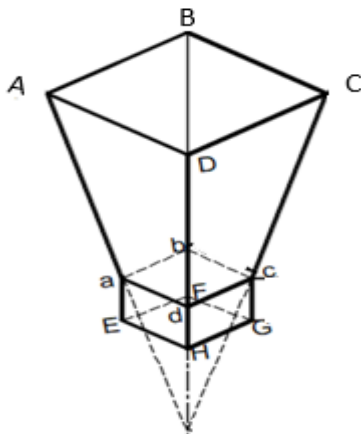


Figure 3: Extractor hopper.

### 2.4.2. Determination of volume of barrel for castor seeds oil extractor

To determine the volume of barrel required for seeds' crushing, the following design parameters are established as follow:

Diameter of press barrel, D<sub>PB</sub> = 70 mm;

Length of press barrel, L<sub>PB</sub> = 900 mm;

Thread (screw winding) breadth, B = 7 mm.

The geometric mean diameter, D<sub>g</sub> of castor seeds ranges between 6.15-11.41 (Isiaka et al., 2012). The thread pitch should be able to accommodate all the ranges of D<sub>g</sub> of castor seeds.

Thread pitch, T<sub>p</sub> = 15 mm;

Considering a tapered screw shaft with outside diameter of 80 mm;

Root diameter of screw shaft at intake = 60 mm

Root diameter of screw shaft at exit = 70 mm

Root diameter of screw winding at midpoint, d<sub>1</sub> = 75 mm;

Thickness of screw winding at intake, t<sub>i</sub> = 10 mm;

Thickness of screw winding at exit, t<sub>e</sub> = 5 mm;

Average thickness of screw winding,  $t = \frac{t_i + t_e}{2} = 7.5$  mm

Length of shaft covered with screw, L<sub>1</sub> = 550 mm

$$\text{Total no. of screw windings on the screw shaft} = \frac{L_1}{B + T_p} \quad (4)$$

The length of a screw winding is determine using the formula for calculating the circumference of a circle. Circumference of a circle =  $\pi d$  (5)

Where;

d is diameter of the circle.

$$\text{Length of a screw winding, } L = \pi \times d \quad (6)$$

For the determination of volume of a screw winding, the formula for calculating the volume of a cuboid was used. Volume of a cuboid = L × B × h (7)

Where;

L, B and h are length, breadth and height or thickness of the cuboid, respectively.

Volume of a screw winding (V<sub>SW</sub>) is obtained as follows:

$$V_{SW} = L \times B \times t \quad (8)$$

In determining the volume of screw shaft (V<sub>SS</sub>) and the inner volume of press barrel, the formula for calculating the volume of a cylinder are used as given in Equation 9.

$$\text{Volume of a cylinder} = \pi r^2 h \quad (9)$$

Where; r and h are the radius and height of the cylinder respectively.

Inner vol. of press barrel (P<sub>b</sub>) occupied by screw shaft + Vol. of 18 screw windings + Vol. of screw shaft considering the root diameter (10)

$$\text{Inner vol. of barrel for castor seeds pressing} = \text{Inner vol. of barrel} - \text{Inner vol. of barrel occupied by screw shaft} \quad (11)$$

Bulk density of castor seeds is considered as 479.23 kg/m<sup>3</sup> (Isiaka et al., 2012). If the volume of castor seeds can be reduced by half (1/2) by crushing and pressing, its bulk density after Pressing, ρ<sub>ba</sub> will be twice of its bulk density before pressing, ρ<sub>bb</sub>. Therefore,

the mass of castor seeds that barrel can accommodate, (which can be expressed as  $M = \rho_{ba} \times \text{Inner vol. of barrel for castor seeds pressing}$ ).

Hence, the crushing (force) strength,  $(FC) = R_f \times S_f$  (12)

Where;

FC is the crushing force

$R_f$  is the rupture force

$S_f$  is the factor of safety

**2.4.3. Power required for moving and rotating of screw shaft**

The power required for continuous moving and rotating of screw shaft can be projected using Equation 13, while the torque developed can be obtained using Equation 14 (Khurmi and Gupta, 2018).

$$P_{RSS} = (2\pi NT)/60 \tag{13}$$

$$T = Fr \tag{14}$$

Where; F, N and r are the weight of screw shaft, screw shaft speed (30 rpm), and radius of screw shaft (0.07/2 m).

**2.4.4. Power required for crushing castor seeds in the press barrel**

The power require for castor seeds crushing is estimated using Equation 15.

$$P_C = FD/t \tag{15}$$

Where F, D and t are force, distance moved and time taken respectively.

**2.4.5. Designs for shaft**

According to Khurmi and Gupta (2018), torque transmitted by a shaft drive given in Equation 16. The maximum permissible shear stress is taken to be 42 MPa for a shaft with allowance for key ways.

$$Tq = \pi/16 \times \tau \times d^3 \tag{16}$$

$$\therefore d = \sqrt[3]{\frac{T \times 16}{\pi \times \tau}} \tag{17}$$

Where: Tq is torque (Nm)

$\tau$  is torsional shear stress (N/m<sup>2</sup>)

d is the diameter of the shaft (m)

**2.4.6. Determination of the crusher axial deflection**

The crusher axial deflection ( $\delta$ ) is estimated using Equation 18

$$\delta = F_c L / AE_m \tag{18}$$

Where:  $\delta$  is axial deflection, (m)

$E_m$  is modulus of elasticity (N/m<sup>2</sup>)

$F_c$  is (crushing force), (N)

A is Area of the crusher, (m<sup>2</sup>)

L is Length of the crusher, (m)

**2.4.7. Determination of the temperature of the heating elements**

Consider three heating elements wound around the crushing chamber as shown in Figure 2 with the following parameter: The Equations 19-22 is according to Yunus and Afshin (2015) and Rajput (2007).

**2.4.8. Determination of heat generated by heaters**

The heat effect produced by an electric current I, through a resistance R, for a time  $T_h$ , is given by;

$$Q = I^2 R T_h \tag{19}$$

Where, Q is Quantity of heat (kW)

R is Resistance ( $\Omega$ )

$T_h$  is the heating Time in second

I is Current in ampere (Amp) and this is estimated as follows:

$$\text{Recall, } P = IV \tag{20}$$

Where, P is Power

I is Current

V is Voltage

Hence,  $I = P/V$

**2.4.9. Determination of heating element capacity**

This is obtained in term of designing for the heater temperature capacity using Fourier law of heat transfer equation given as follows:

$$Q = k A \Delta T / L \tag{21}$$

Where:

$\Delta T$  is temperature change (K)

L is the length (m)

k is thermal conductivity of the drum material (W/m·K)

**2.4.10. Heat transfer by convection**

It is also necessary to calculate the heat transfer from the surface to the air. This is done by using convective heat transfer relation given as:

$$Q = hA \Delta T \tag{22}$$

Where:

Q is Rate of heat transfer (w)

h is Convective heat transfer coefficient (W/m<sup>2</sup>-K)

A is Surface area for heat transfer (m)

$\Delta T$  is the temperature change.

**2.4.11. Machine fabrication procedures**

Various fabrication processes used in the fabrication of machines that make up the extractor include but not limited to;



- i Market survey of the selected materials and costing,
- ii Materials procurement,
- iii Measurement and making out exercise,
- iv Cutting of parts to required sizes,
- v Forming operation, which has to do with bending and rolling of required machine components to geometrical shapes and sizes.
- vi Machining: This involves drilling, cutting of various machine parts, blanking, piercing and turning of shafts.
- vii Joining Operation: the joining process of the machine fabrication involved welding of parts (using electric arc welding) and fastening through the use of bolts and nuts and well as screwing.
- viii Grinding and surface finishing,
- ix Assembling of the fabricated machines section by section
- x Painting of machine frames and other machine components that needed to be painted. The painting is necessary in order to increase the aesthetic view and market-ability of the developed plant.
- xi Incorporation of heater element and control devices in order to automate the operations of the extractor. This is the last phase of the extractor development,

Tools and equipment used for the fabrication work include but not limited to; meter rule, vernier caliper, scribe, hacksaw, table vice, welding machine, grinding machine, bending/rolling machine, spanners and screw driver, hammer and spanners of different sizes.

**2.4.12. Determination of machine throughput capacity and efficiency**

The machine throughput capacity, time and efficiency are determined by using Equations 23-25 respectively (Orhororo et al., 2016; Oyejide et al., 2018).

$$MTC = M/T \tag{23}$$

Where:

MTC is machine throughput capacity (kg/min)

M is mass of castor seeds (kg)

T is time taken to extract castor oil (min.)

The efficiency is given by Equation 24.

$$Eff.=MDM/MT \tag{24}$$

Where:

MDM is mass of extracted oil from castor oil seeds (Developed Machine)

MT is total mass of castor seeds oil.

Hence, the average efficiency, mass of castor seeds oil, processing time are calculated from Equation 25.

$$Ave = \epsilon/n \tag{25}$$

Where;

Ave is the average of the sum of all the values divides by the total number.

$\epsilon$  is the summation of the number.

n is the total number of tests (ref. to Table 1). Table 1 shows the results obtained from the deduction in the Equations 23-25 respectively.

Where:

M(HI) is the mass of castor oil obtained from the machine with heat element incorporated (kg)

T(HI) is the time required to extracted mass of the castor oil from the machine with heat element incorporated (min)

M(WHI) is the mass of castor oil obtained from the machine without heat element incorporated (kg)

T(WHI) is the time required to extracted mass of the castor oil from the machine without heat element incorporated (min).

**2.4.13. Determination of output capacity**

This is the rate of castor seed extraction in kg/h. It is the ratio of the weight of castor seed extracted to the total time taken to extract the castor seed. It was determined using Equation 26.

$$C_o = We/T \tag{26}$$

Where:

$C_o$  is output capacity (kg/h)

**Table 1.** Results of mass of oil extracted, time, machine throughput capacity and efficiency.

S/N	Developed machine with heat element incorporated					Developed machine without heat element incorporated				
	M(T) (kg)	M(HI) (kg)	T(HI) (min)	M(TC) (kg/min)	Eff. (%)	M(WHI) (kg)	T(WHI) (min)	MTC (kg/min)	Eff.(%)	
1	6.00	3.30	4.40	1.36	55	1.89	6.10	0.983	32	
2	7.00	4.00	5.35	1.31	57	2.00	7.30	0.959	29	
3	8.00	4.60	6.30	1.27	58	2.36	10.05	0.796	30	
4	9.00	5.30	7.00	1.26	59	2.70	13.15	0.631	33	
5	10.0	6.10	8.00	1.25	61	3.90	15.10	0.627	41	

**Table 2.** Summation and average MTC, Time and Efficiency.

$\epsilon$	40	23.3	31.05	6.45	290	12.85	51.7	3.996	165
Ave	8	4.66	6.21	1.29	58	2.57	10.34	0.7992	33

We is mass of castor seed (kg)

T is total time taken for extraction (h)

### 3. Results and Discussions

#### 3.1. Simulation results

The simulation of the designed machine was done to determine the manufacturability, functionality and the structural stability of the design prior to fabrication. The Finite Element Analysis (FEA) of the castor oil extracting machine's extrusion screw as presented in Figure 4 provides valuable insights into its structural behaviour under applied loads as follow:

##### 3.1.1. Deformation analysis of the extracting machine's extrusion screw

The FEA results for the castor oil extracting machine's screw reveal crucial insights as presented in Figure 4. The maximum deformation at the middle of the screw ( $4.24 \times 10^{-4}$  mm) signifies localized response to loads, potentially indicating stress concentrations. In contrast, the negligible deformation at the end of the screw ( $6.253 \times 10^{-12}$  mm) aligns with operational expectations. The average deformation ( $2.10 \times 10^{-4}$  mm) reflects minimal displacement across the screw, contributed to overall stability of the machine's screw. Analyzing spatial deformation distribution helps identify critical areas for potential design modifications or reinforcement. Ensuring deformations meet design limits and industry standards confirms the screw's structural performance within acceptable criteria. These findings guide designers in optimizing the screw's behaviour for efficient operation of the designed castor oil extracting machine. The result of this investigation is linked with that in the studies of Ojo et al., (2022) with maximum value of washing machine's spindle shaft deformation of  $3.45 \times 10^{-4}$  mm.

##### 3.1.2. Stress analysis of the extracting machine's extrusion screw

The stress analysis of the castor oil extracting machine's screw provides vital information about its mechanical response to applied loads as shown in Figure 5. The maximum stress is  $5.26 \times 10^{-1}$  MPa at the screw's connection to the motor, signifies a critical region with potentially higher loading conditions. The minimum stress is very low at 15.174 Pa at the opposite end, suggests minimal mechanical loading in that area. The average stress of  $5.20 \times 10^{-2}$  MPa offers an overall measure of stress distribution, indicating the screw's general mechanical behaviour. Spatially, examining stress distribution along the screw's length helps identify critical regions and potential points of failure. Comparing stresses with design limits and industry standards ensures the screw's mechanical performance aligns with safety criteria. The findings guide designers in optimizing the screw's structural integrity, confirming its suitability for the intended application in the castor oil extracting machine. Careful consideration of stress concentrations and variations inform potential design modifications or reinforcements for enhanced mechanical performance. The achieved results in this study agreed with that obtained in the studies of Ojo et al., (2022) having washing machine's spindle shaft stress of  $6.34 \times 10^{-2}$  MPa.

##### 3.1.3. Strain analysis of the extracting machine's extrusion screw

The strain analysis of the castor oil extracting machine's screw (Figure 6) reveals critical information about its strain distribution under applied loads. The maximum strain, at  $3.6133e-6$ , occurring at the hole where a bolt couples the screw and motor, suggests concentrated deformation in this region. This could be due to the high stress associated with the coupling point. The minimum strain of  $7.6153e-011$  at the other end indicates

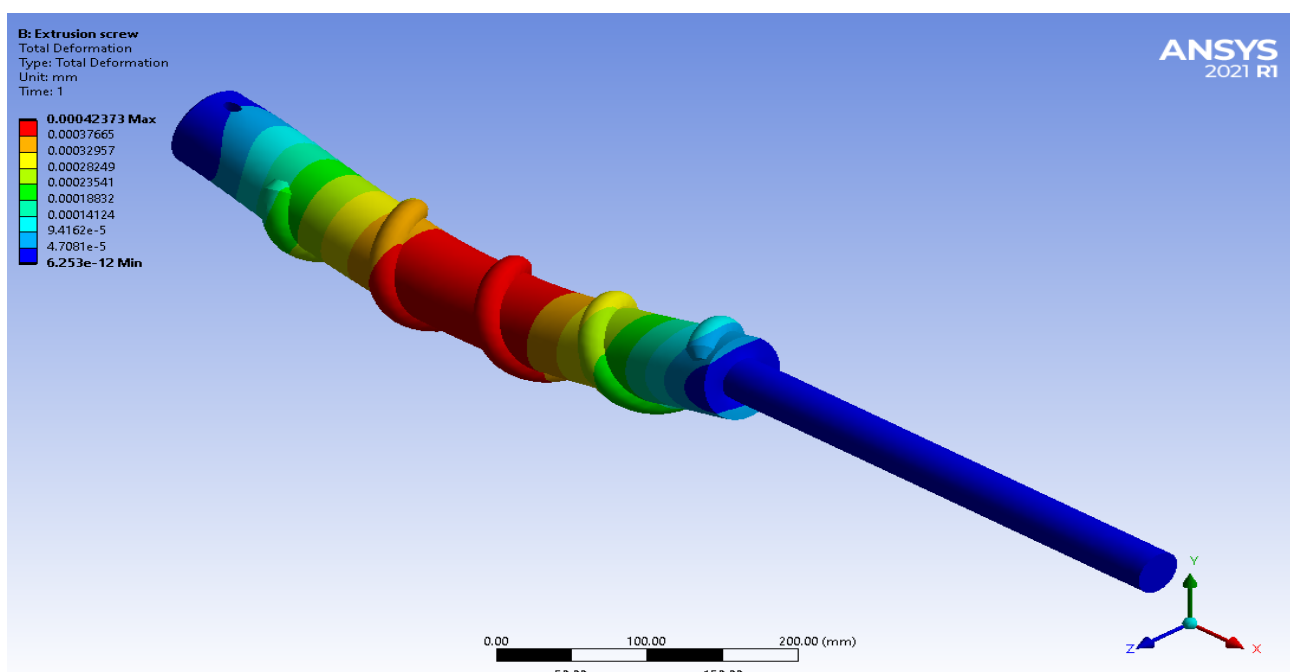


Figure 4: FEA simulation result of the deformation of the screw shaft.

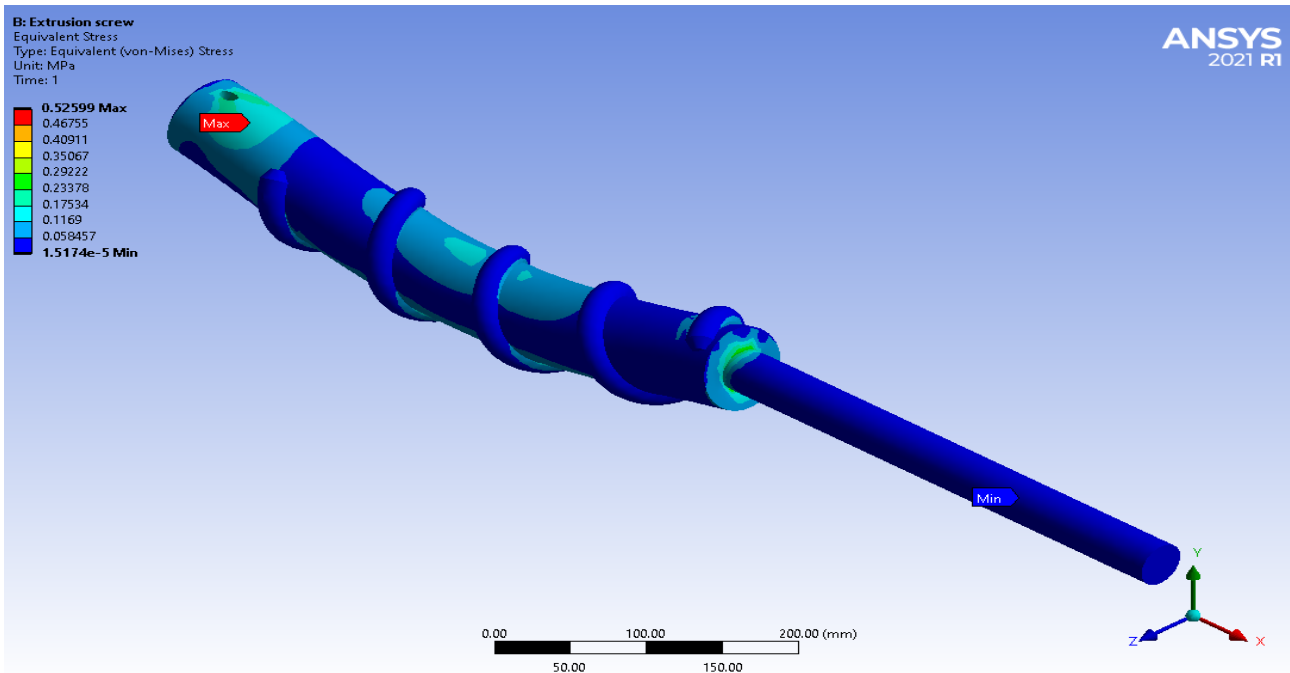


Figure 5: FEA simulation stress result of the screw.

negligible deformation, likely influenced by boundary conditions or reduced mechanical loading. The average strain, at  $2.7927e-007$ , provides an overall measure of strain distribution, indicating the screw's general response to applied forces. Analyzing strain results aids in understanding localized deformation patterns, guiding potential design modifications or reinforcements to optimize the screw's structural integrity for efficient operation in the castor oil extracting machine. The result

of the strain analysis is comparable with that achieved in the studies of Ojo et al., (2022) with obtained value of washing machine's spindle shaft strain of  $3.2125e-007$ .

### 3.1.4. FEA determination of the designed castor oil extraction machine Factor of safety

The factor of safety (FOS) for the steel screw in the castor oil extracting machine, with a tensile yield strength of 250 MPa and a maximum stress of 52.599 MPa, is

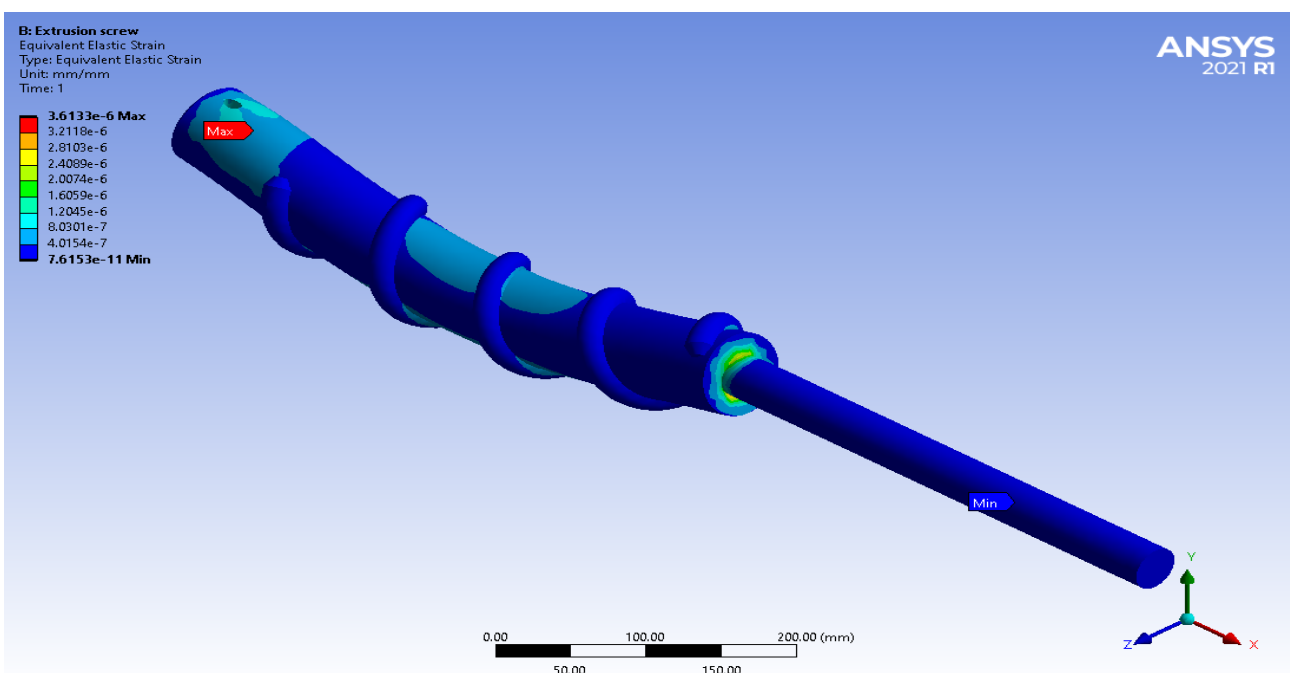


Figure 6: FEA simulation strain result.



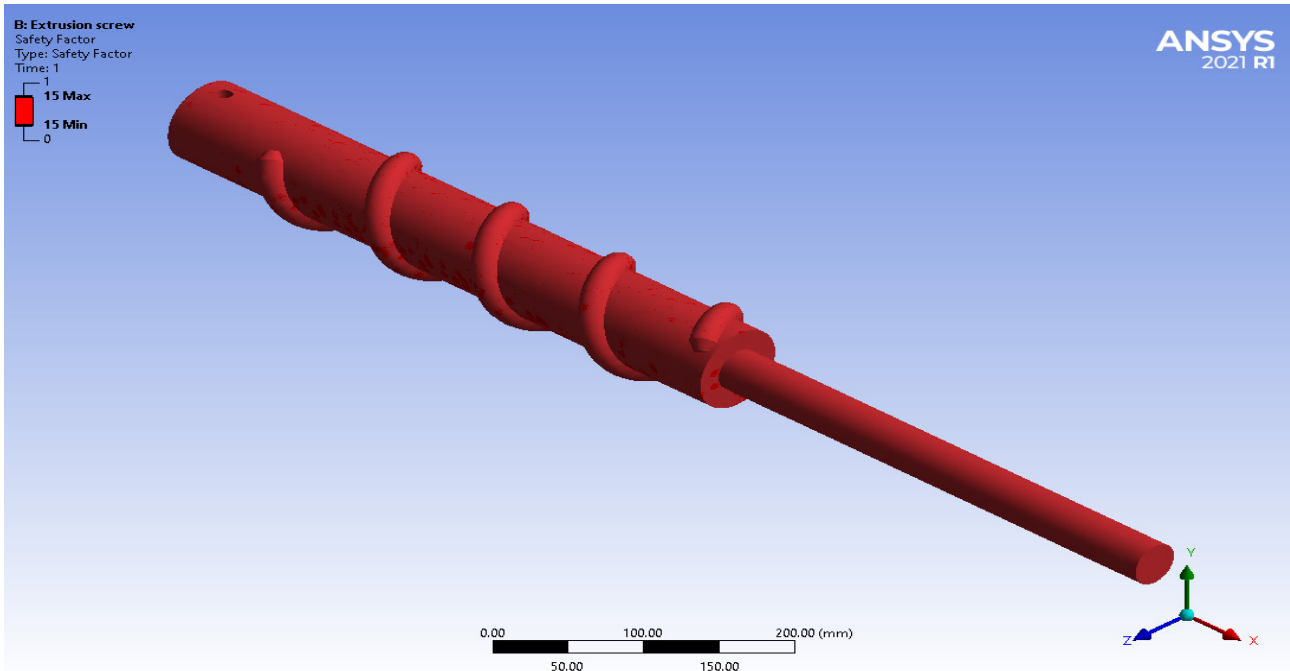


Figure 7: FOS simulation result.

approximately 15 as depicted in Figure 7. This high factor of safety indicates a substantial margin between the material's capacity to withstand loads and the applied stress, ensuring the screw's structural integrity. The FOS of 15 suggests that the steel screw is well within its elastic limits and can safely withstand the analyzed stress conditions, providing confidence in its performance and durability in the castor oil extracting machine. This result is comparable with that in the studies of Ojo et al., (2022) with the obtained value of FOS of 4 in the analysis of washing machine's spindle shaft.

### 3.2. Results of finite element analysis of the frame

The FEA of the castor oil extracting machine's frame provides valuable insights into its structural behavior under applied loads.

#### 3.2.1. Deformation analysis of the extracting machine's frame

The FEA results for the frame in the castor oil extracting machine presented in Figure 8 revealed significant deformation patterns. As can be noticed in the figure, the

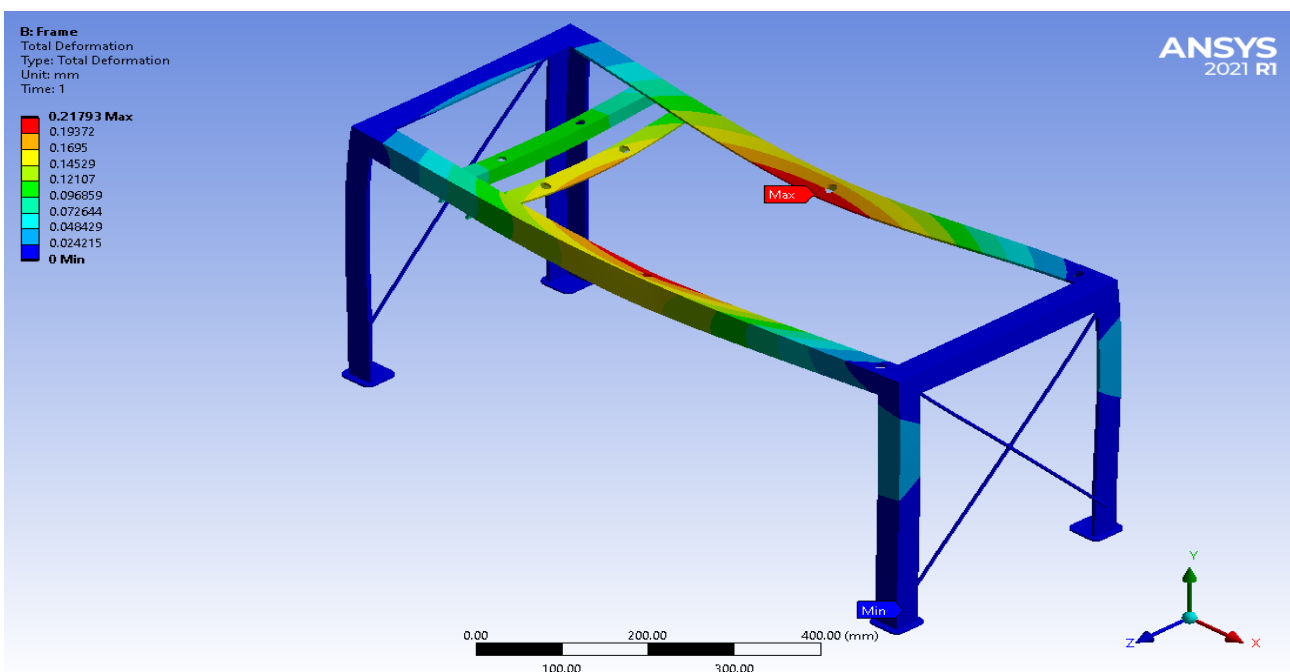


Figure 8: FEA result of the deformation of the frame.

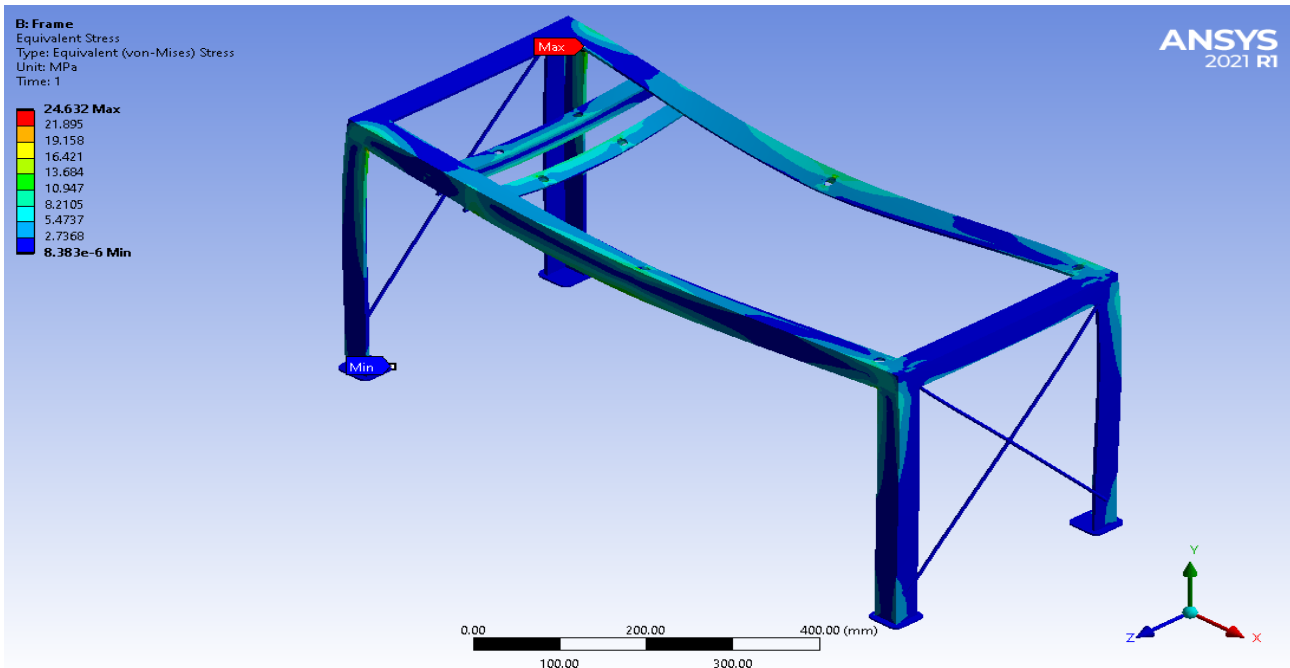


Figure 9: FEA simulation stress result of the frame.

maximum deformation, occurring at  $2.18 \times 10^{-1}$  mm in the middle of the longest bar, indicates the most substantial displacement, highlighting a critical region for potential stress concentrations. The minimum deformation of 0 mm at the legs suggests negligible displacement, likely influenced by boundary conditions or reduced mechanical loading. The average deformation of  $5.25 \times 10^{-2}$  mm provides an overall measure of the frame's response to applied loads, indicating its general structural behaviour. Spatially analyzing deformation distribution offers insights into localized patterns, guiding attention to areas requiring potential design modifications or reinforcement. Assessing these deformation results ensures that the frame aligns with design expectations and industry standards, optimizing its structural integrity and stability in the castor oil extracting machine. This result is comparable with that attained in the studies of Ojo et al., (2022) with maximum deformation value of  $3.22 \times 10^{-2}$  mm in the analysis of washing machine's frame.

### 3.2.2. Stress analysis of the extracting machine's frame

The stress analysis of the frame in the designed castor oil extracting machine reveals critical findings. The maximum stress of 24.632 MPa concentrates at the corner joint of the slender part, emphasizing a potential vulnerability. In contrast, the minimum stress of 8.383e-006 MPa at the base of the legs shown in Figure 9 suggests minimal mechanical loading in that region. The average stress of 2.4094 MPa provides an overall measure of stress distribution. Spatially, examining stress patterns aids in identifying critical regions. Design considerations is ensuring that the maximum stress aligns with material capacity and

application requirements. This result is comparable with that in the literature of Ojo et al., (2022) having washing machine's frame stress value of 25.777 MPa.

### 3.2.3. Strain analysis of the extracting machine's frame

The strain analysis of the frame in the castor oil extracting machine provides valuable insights into its deformation under applied loads. The maximum strain, reaching  $1.37 \times 10^{-4}$  at the corner joint where the longest bar connects to the legs, indicates concentrated deformation at a critical junction shown in Figure 10. This insight is essential for understanding potential stress concentrations and load-bearing characteristics. The minimum strain of  $4.2105e-011$  at the base of the legs suggests minimal deformation in this area, likely influenced by boundary conditions or reduced mechanical loading. The average strain of  $1.33 \times 10^{-5}$  provides a comprehensive measure of the frame's overall deformation response. The design considerations of the frame are assessed to ensure that the strain values align with safety margins and intended functionality, guiding potential modifications or reinforcements for optimal structural performance and stability in the castor oil extracting machine. This result is comparable with that in the study of Ojo et al., (2022) having washing machine's frame strain analysis of  $2.12 \times 10^{-5}$ .

### 3.2.4. FEA determination of factor of safety for the designed oil extraction machine frame

The FOS is a critical metric in assessing the reliability of a steel frame in the castor oil extracting machine. With a tensile yield strength of 250 MPa and a

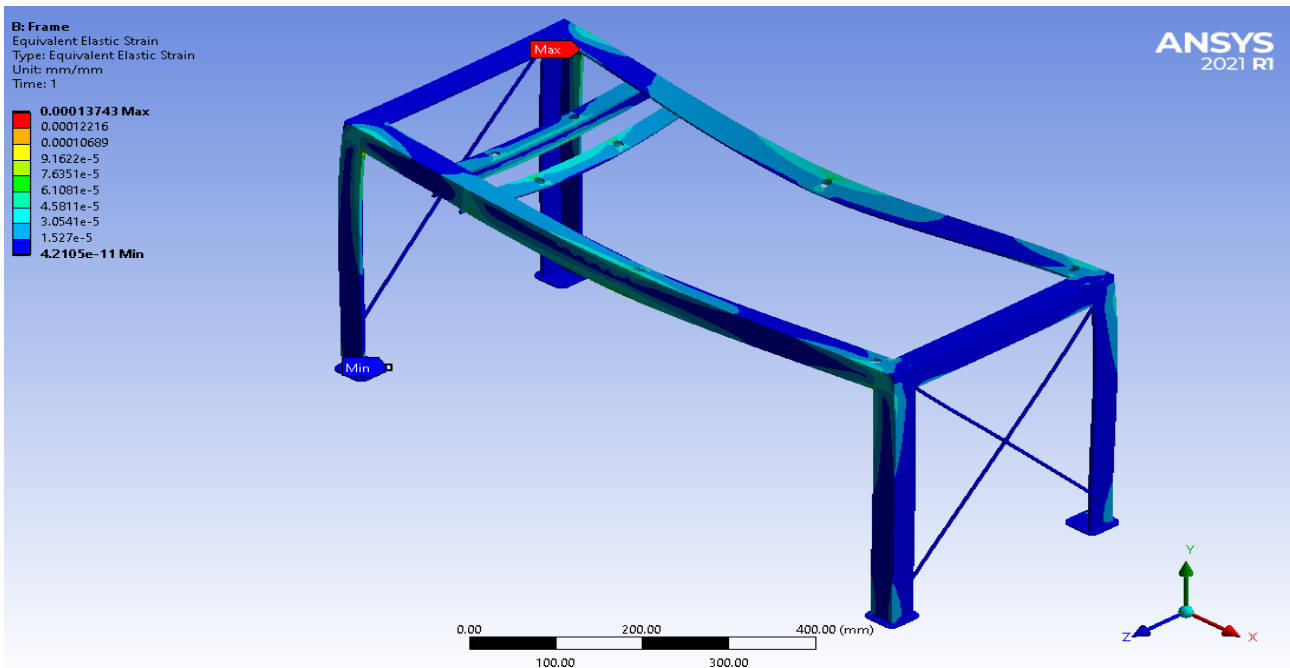


Figure 10: FEA Simulation strain result.

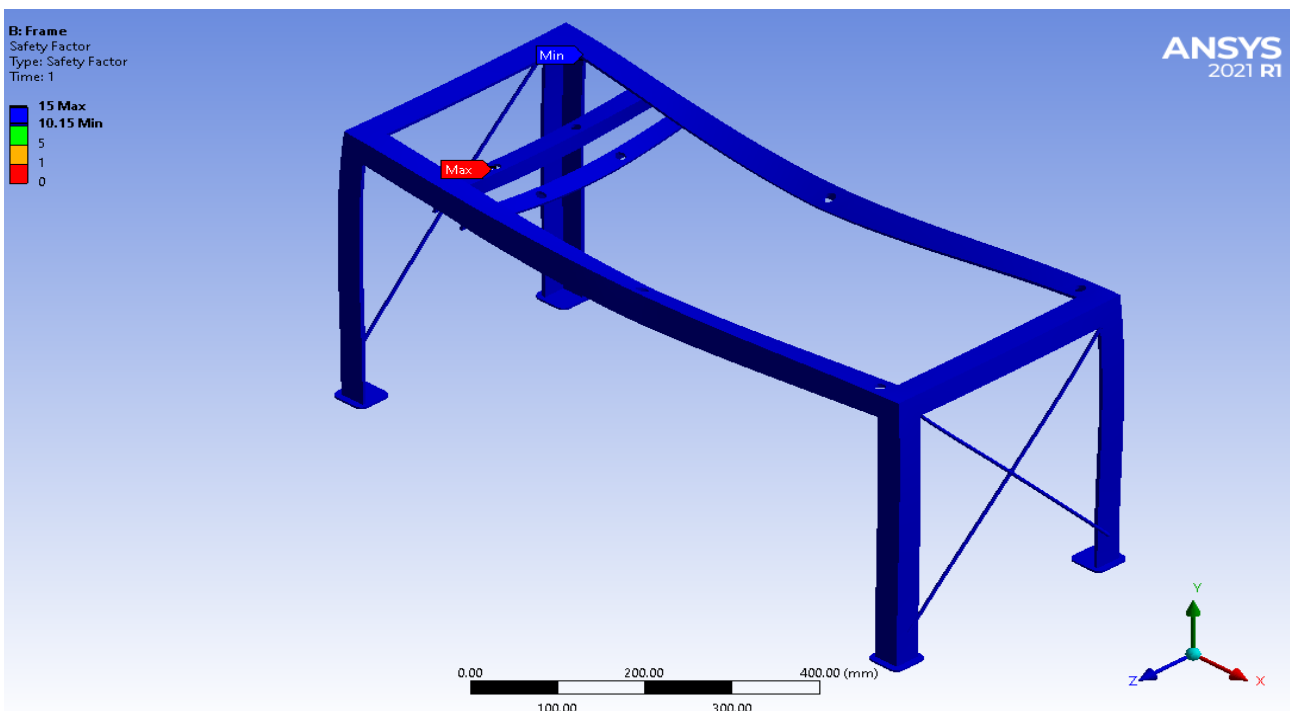


Figure 11: FOS simulation result.

maximum stress of 24.632 MPa. The calculated FOS is 10.15 using Equation 27 is found the same with the simulated value shown in Figure 11.

$$FOS = \frac{250}{24.632} = 10.1 \quad (27)$$

A higher FOS, in this case, signifies a considerable margin of safety, providing confidence in the frame's ability to withstand applied loads. Achieving a well-balanced FOS of 10.15 ensures the steel frame's

structural integrity and operational safety under various conditions. This result is comparable with that in the study of Ojo et al., (2022) with obtained value of FOS of 5 for washing machine's frame.

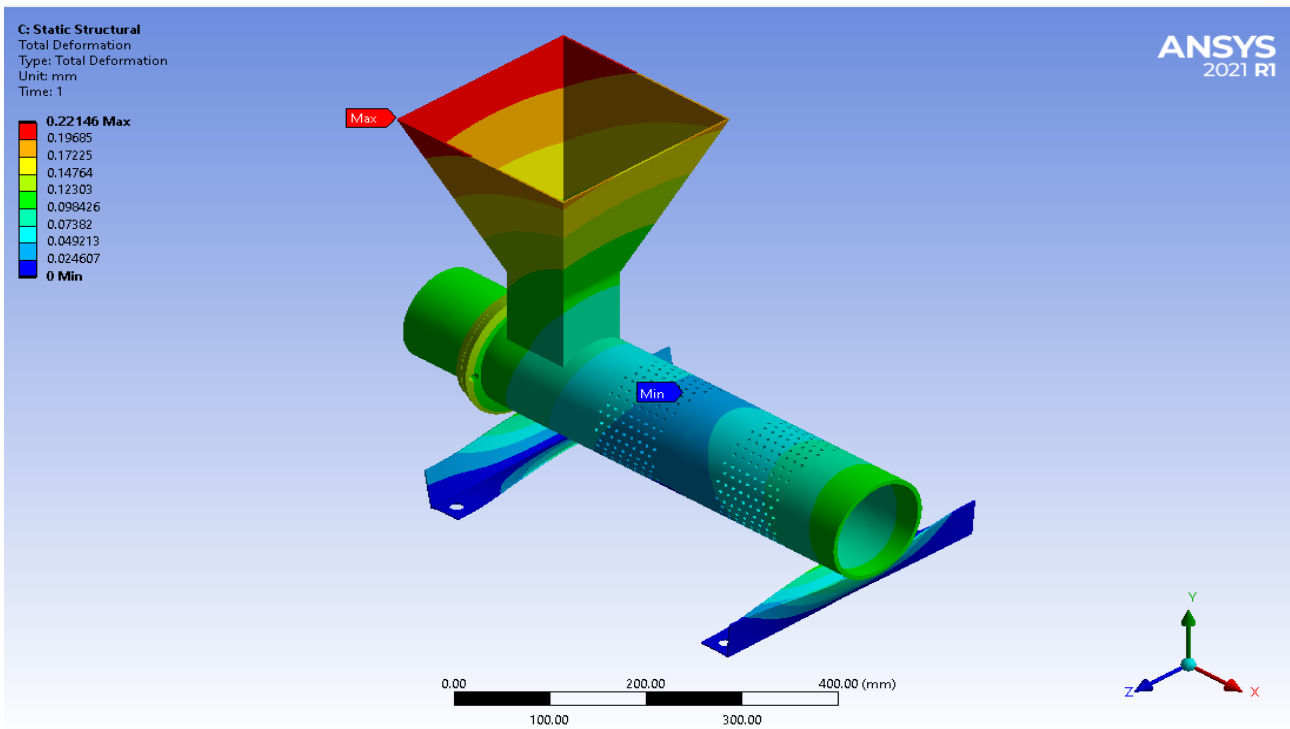


Figure 12: FEA simulation result of the deformation of the housing for the feeding screw shaft and heating unit.

### 3.3. Results of finite element analysis of the housing for feeding screw and heating unit

#### 3.3.1. Deformation analysis of the housing for feeding screw and heating unit

The deformation analysis of the housing for the feeding screw shaft and heating unit presented in Figure 12

reveals critical insights. The maximum deformation of  $2.21 \times 10^{-1}$  mm, observed at the edge of the feeding hopper, signifies a notable displacement point. Identifying this location is essential to understanding potential stress concentrations, ensuring the housing can withstand applied loads in this critical region. In contrast, the minimum deformation of 0 mm at the middle of the crushing

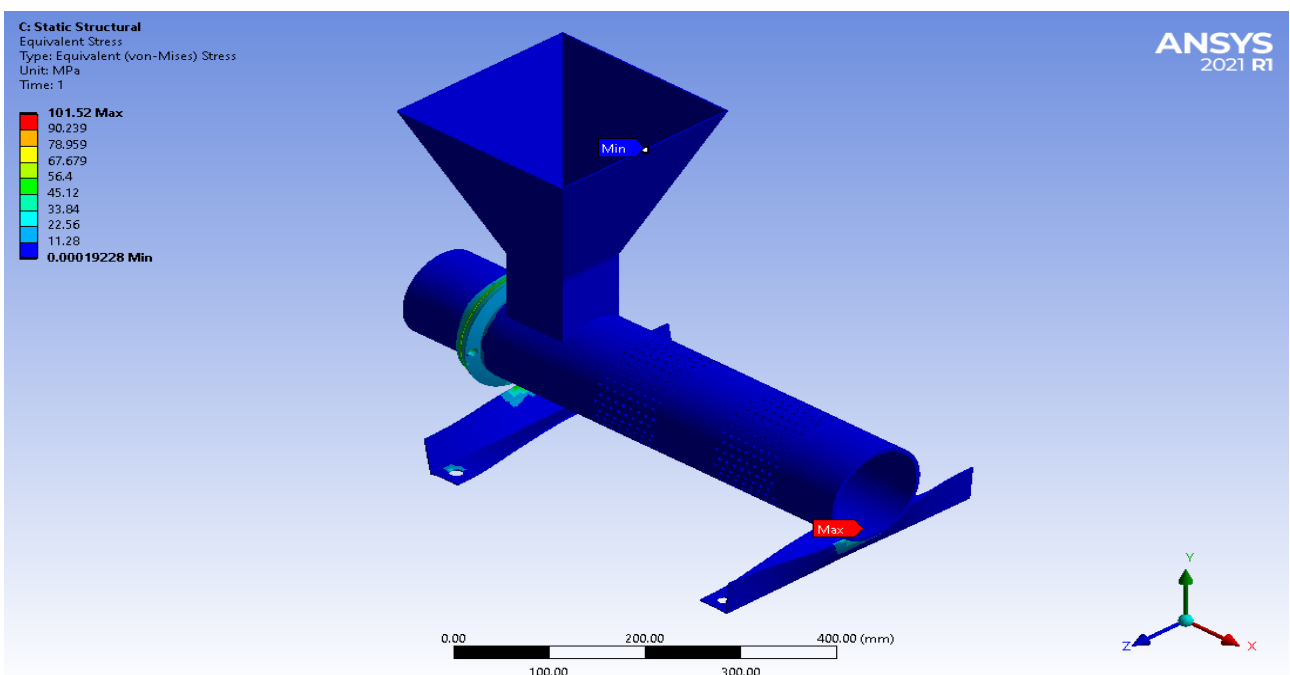


Figure 13: FEA stress result of the housing for the feeding screw shaft and heating unit.

chamber indicates minimal displacement, potentially influenced by constraints or reduced mechanical loading in this area. The average deformation of  $5.857e-002$  mm provides a comprehensive measure of the housing's overall structural response. Evaluating spatial distribution helps pinpoint areas with higher or lower deformations, guiding potential design modifications or reinforcements for optimized structural performance and stability in the castor oil extracting machine. This result is comparable with that in the studies of Ojo et al., (2022) with the value of  $3.11 \times 10^{-1}$  mm for the analysis of washing machine's feeding screw.

**3.3.2. Stress analysis of the housing for feeding screw and heating unit**

The stress analysis for the housing of the feeding screw shaft and heating unit provides crucial information for structural evaluation. The maximum stress, reaching 101.52 MPa at the end joint of the shaft housing and the motor sleeve obtained in Figure 13, signifies a critical point where intense forces are concentrated. This area demands special attention to prevent potential structural failure. Conversely, the minimum stress of  $1.92 \times 10^{-4}$  MPa at the other end of the shaft housing suggests a relatively low-stress region, potentially influenced by reduced mechanical loading. The average stress of 1.4776 MPa provides an overall measure of stress distribution. Design considerations should ensure that the maximum stress aligns with material capacity, while potential design modifications or reinforcements may be necessary to optimize structural performance and safety in the castor oil extracting machine. This result is comparable with that in the study of Ojo et al., (2022) having value of  $2.22 \times 10^{-4}$  MPa for the machine's feeding screw stress.

**3.3.3. Strain analysis of the housing for feeding screw and heating unit**

The strain analysis for the housing of the feeding screw shaft and heating unit unveils critical deformation patterns. The maximum strain of  $5.15 \times 10^{-4}$  depicted in Figure 14, concentrated at the end joint of the shaft housing and the motor sleeve, indicates a notable deformation point requiring careful consideration for potential stress concentrations. In contrast, the minimum strain of  $8.6593e-009$  at the edge of the feeding hopper suggests minimal deformation in this region. The average strain of  $9.231e-006$  provides a comprehensive measure of the housing's overall deformation response. Engineers should assess whether these strain values align with safety margins and intended functionality, guiding potential modifications or reinforcements for optimal structural performance and stability in the castor oil extracting machine. This result is comparable with that in the study of Ojo et al., (2022) with obtained value of  $4.47 \times 10^{-4}$  for the washing machine's strain.

**3.3.4. FEA determination of factor of safety for the designed oil extraction machine housing and heating units**

The FOS for the housing of the feeding screw shaft and heating unit, constructed from a steel sheet with a tensile yield strength of 250 MPa, is crucial for assessing structural reliability. With a maximum stress of 101.52 MPa in the housing, the calculated FOS is obtained by dividing the yield strength by the maximum stress as follow:

$$FOS = \frac{250}{101.52} = 2.46 \tag{28}$$

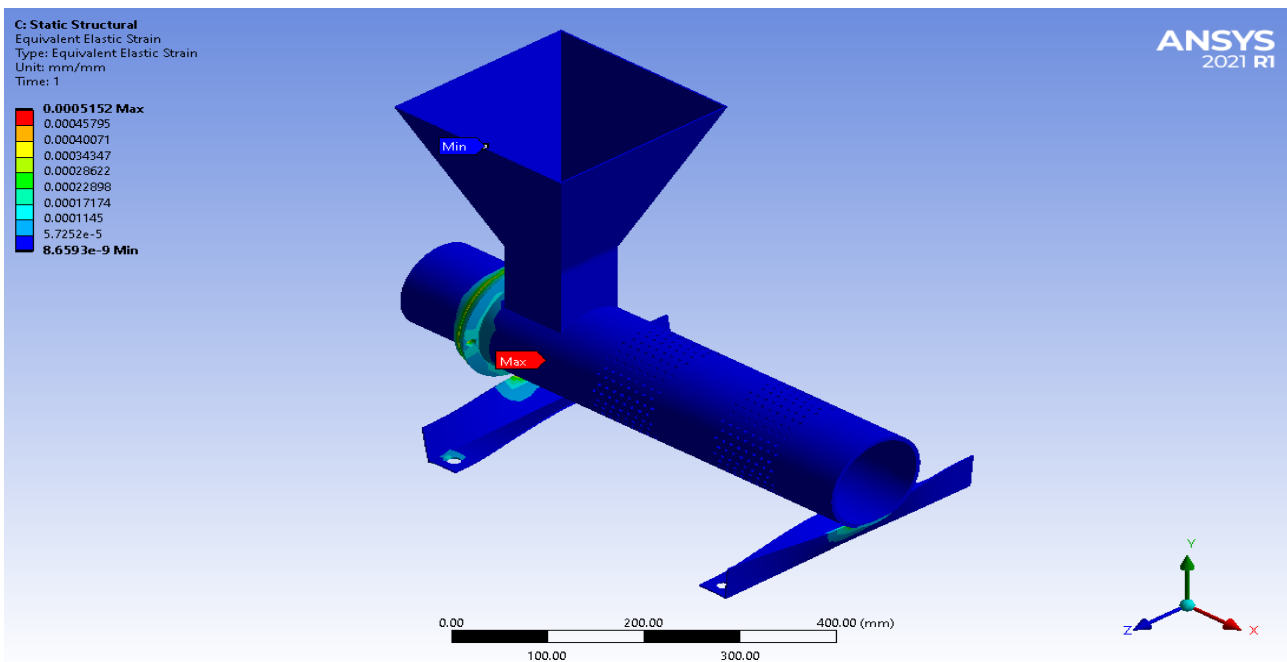


Figure 20: Strain result

Figure 14: FEA strain result of the housing for the feeding screw shaft and heating unit.



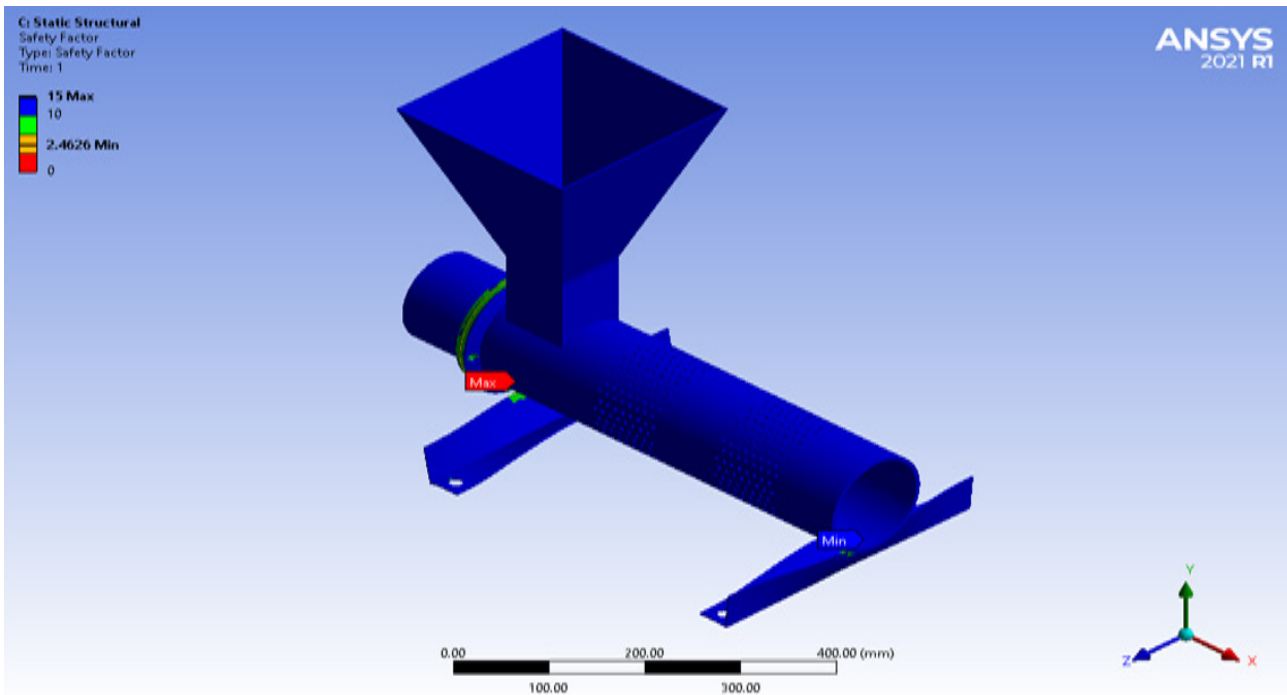


Figure 15: FOS simulation result of the housing for the feeding screw shaft and heating unit.

With a tensile yield strength of 250 MPa, the FOS is calculated as the ratio of this strength to the maximum stress experienced by the housing, which is 101.52 MPa. A higher FOS of about 2.46 shown in Figure 15 and similar to the calculated value using Equation 28 indicates a greater margin of safety against potential structural failure. This result is comparable with that in the study of Ojo et al., (2022) with value of FOS of 3 in the analysis of washing machine’s feeding screw.

### 3.4. Result of the machine throughput capacity, mass of castor oil extracted, time and efficiency

The results of machine throughput capacity, mass of castor oil extracted, time and efficiency obtained with the developed castor seeds oil extractor machine and machine of similar capacity without heat element incorporated are presented in the Figures 16 - 19. The obtained machine throughput capacity, Mass of castor oil extracted and efficiency of the oil extractor machine in this study are estimated using Equations 23 - 25.

Figure 16 shows the obtained machine throughput capacity of the developed oil extractor machine in this study. The mass of castor seeds charged into the machine in relation to the processing time were used to calculate the machine throughput capacity. The machine was fed with following mass of castor seeds at each stage of testing; 6, 7, 8, 9 and 10 kg respectively. The results obtained show that better machine throughput capacity was obtained with machine with heat element incorporated (MWHIC). However, an average throughput capacity of 1.29 kg/minutes was obtained with the developed machine with heat element incorporated (MWHIC) against one without heat element incorporated (MWOHIC) of value 0.710 kg/minutes. The

result of machine throughput capacity is comparable with that in the literature of Oyejide et al., (2018) with the value of machine’s throughput capacity of 0.238 kg/minutes.

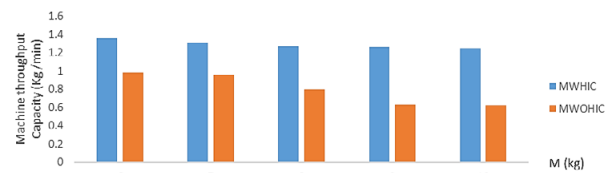


Figure 16: Machine throughput capacity versus mass of castor seeds.

Presented in Figure 17 is the graph of mass of castor oil obtained from developed castor seeds extraction machine with heat element incorporated (MWHIC) and similar machine of the same capacity without heat element incorporated (MWOHIC). The machine was fed with following mass of castor seeds at each stage of testing; 6, 7, 8, 9 and 10 kg respectively. The results obtained show that the output gotten from developed machine with heat element incorporated (MWHIC) was higher than the one without heat element incorporated (MWOHIC) in oil extraction from the castor seeds. Additionally, the obtained average oil yield of 4.66 kg for machine with heat element incorporated (MWHIC) in comparison to 2.57 kg for machine without heat element incorporated (MWOHIC) was recorded (refer to Table 2). The continuous increase in quantity of castor oil in respect to mass of castor seeds fed into the machine as shown in the figure confirmed better machine of the machine with heat element incorporated (MWHIC) developed in this research. The result of mass of extracted castor oil is comparable with that observed in the study of Oyejide et al., (2018) having mass of extracted oil of 2.23 kg.

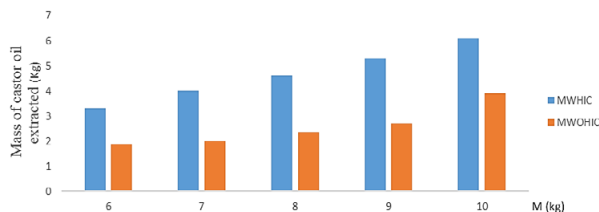


Figure 17: Mass of oil extracted against mass of castor seeds.

Figure 18 shows the graph of time required to process castor oil in relation to the mass of castor seeds obtained. The same mass of castor seeds was fed into the machine at each stage of testing; 6, 7, 8, 9 and 10 kg respectively. The results indicate that processing with developed machine with heat element incorporated (MWHIC) was faster and yield higher oil than the similar machine without heat element incorporated (MWOHIC) as shown in the figure, this because the heater element has raised the temperature of moisture content in the castor seeds. It can be seen from the figure that as the mass of castor seeds fed into the machine increases the processing time also increased. Observations from the Table 2 indicated that, with the average mass of 8kg of castor seeds fed into the developed machine with heat element incorporated (MWHIC), it required average processing time of 6.21 min to extracted castor oil of 4.66 kg compared to machine without heat element incorporated (MWOHIC) with the same of 8 kg mass of castor seeds, it took 10.34 min to extracted oil of 2.57 kg. The result of time required to process castor oil is comparable with that in the literature Oyejide et al., (2018), taking 85 min. to extracted oil of 5.23 kg.

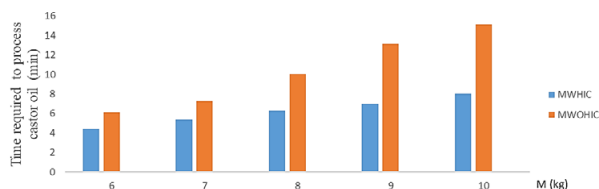


Figure 18: Time required to process castor oil against mass of castor seeds.

Figure 19 presents the result of machine efficiency versus mass of oil obtained in this study. Efficiency of a machine is an indication how well the input variable is converted to useful output. From the Table 2, observation revealed that the efficiency of the machine after fed with average mass of 8 kg of castor seed, results obtained were 4.66 kg castor oil extracted and 58% for developed machine with heat element incorporated (MWHIC) against 2.57 kg castor oil extracted and 33% of the machine without heat element incorporated (MWOHIC). From the Fig., the developed machine with heat element incorporated (MWHIC) is more efficient than the one without heat element incorporated (MWOHIC). Also, at each stage of testing, improved efficiency was achieved with the machine. This is an

indication that the machine performance is satisfactory. The result of efficiency of the machine is comparable with that in the study of Oyejide et al., (2018) having machine efficiency of 46.7%. The machine's efficiency was slightly higher than later as a result of heat element incorporation in the extracting chamber of the machine. However, the performance of the machine could be further enhanced by reducing the extracting chamber's volume, thereby increasing the pressure, hence improving oil yield by maximizing contact between the solvent and castor seeds. Additionally, reducing friction in the machine's rotating parts can also boost overall efficiency.

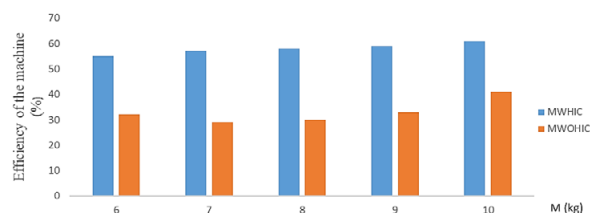


Figure 19: Efficiency against mass of castor seeds

#### 4. Conclusion

This work presents the design and FEA of a castor oil extractor for the production of castor biodiesel. The FEA analysis of the screw shaft in the designed machine revealed a maximum stress distribution of  $5.26 \times 10^{-1}$  MPa, which is below the yield strength of 460 MPa for the selected material. The maximum deformation under loading conditions is  $4.24 \times 10^{-4}$  mm, which is negligible and does not lead to any failure or reduction in the lifespan of the screw shaft. The results from the design calculations and simulation of machine components provided the necessary information required for successful fabrication of the machine. The designed machine can function independently for extracting castor oil. It can also be used to extract oil from other seed plants as long as they are similar in size to castor seeds, thereby reducing the challenges associated with conventional extracting machines. The use of worm gears in the motor allows for high transmission efficiency, resulting in energy savings. With a wide range of applications, the castor oil extraction machine can also process peanuts, sunflower seeds, camellia seeds, cotton seeds, and more. This versatility would increase the machine's scientific and commercial value.

#### Acknowledgements

The authors are thankful to Engr Ogunwole Adeshola Oladepo and Sunday Omodare of the Air Force Institute of Technology, Kaduna, Nigeria for their guidance and support during the fabrication process.

#### References

- Adewale, P., Dumont, M.J., & Ngadi, M. (2016). Enzyme-catalyzed synthesis and kinetics of ultrasonic assisted methanolysis of waste lard for biodiesel production. *Chemical Engineering Journal*, (284), 158–165. <https://doi.org/10.1016/j.cej.2015.08.053>
- Ali, M., Watson, I. (2014). Comparison of oil extraction methods, energy analysis and biodiesel production from flax seeds. *International Journal of Energy Research*, (38), 614–625. <https://doi.org/10.1002/er.3066>

- Azeez, N.A., Okpara, I.N., & Ologunye, O.B. (2019). Design and Fabrication of Sugarcane Juice Extractor. *American Journal of Engineering Research (AJER)*, 8 (7), 91-97.
- Chibuye, B., Singh, S.I., Chimuka, L., Maseka, K.K. (2023). A review of modern and conventional extraction techniques and their applications for extracting phytochemicals from plants. *Journal of scientific African*, (19), 01585. <https://doi.org/10.1016/j.sciaf.2023.e01585>
- Ejiroghene, K.O. (2021). Design of a multi-purpose crushing machine for processing of food grains in Nigeria. *Afribary.com*: Retrieved May 15, 2021, from <https://afribary.com/works/design-of-a-multi-purpose-crushing-machine-for-processing-of-food-grains-in-nigeria> (accessed 13 January 2024).
- Fadhil, A.B., Aziz, A.M., & Al-Tamer, M.H. (2016). Biodiesel production from Silybum marianum seed oil with high free fat acid content using sulfonated carbon catalyst for esterification and base catalyst for transesterification. *Energy Conversion Management*, (108), 255–265. <https://doi.org/10.1016/j.enconman.2015.11.013>
- Fatima, A., Ikram, H., Saleha, I.R., Azka, S.M., Sumbal, S.Q., Amna, A., Fatima, I.S. (2022). Current trends in biodiesel production technologies and future progressions: A possible displacement of the Petro-diesel. *Journal of Cleaner Production*, (370), 133479. <https://doi.org/10.1016/j.jclepro.2022.133479>
- Habib, U., Dipayan, M., & Shahidul, H. (2016). Design and construction of oil expeller press with structural analysis of screw with Ansys. In: International Conference on Mechanical Industrial and Energy Engineering. Khulna, Bangladesh.
- Isiaka, M., Ndon, E., Muhammed, S., & Abdulsalam, M. (2012). Design related physical properties of castor seeds. *Research Journal of Applied Sciences, Engineering and Technology*, 4(23), 5157-5161.
- Jour, T., Barajas, A., & Carman, P. (2004). Biodiesel from castor oil: A promising fuel cold weather. *Journal of Renewable Energy and Power Quality*, 1 (10), 24084.
- Ketan, S.T., Yashodip, K.C., Akshay, R.K., Shailesh, K., & Praveen, K.M. (2017). Design and development of groundnut oil extracting machine by human pedal flywheel motor concept. *International Research Journal of Engineering and Technology*, 4(1), 56 – 72. <https://doi.org/10.22161/ijaers.4.1.11>
- Khurmi, R.S., & Gupta, J.K. (2018). *A Textbook on Machine Design*, Fourteenth Edition; Eurasia Publishing House (PVT.) Ltd. P.512-513.
- Krishna, K.H., Hanock, S., Dsouza, N., & Satheesh, K. (2016). Investigation of properties of different blends of castor and pongamia biodiesels and their performance in a compression ignition engine. *Journal of Energy and Power*, 6(1), 8-14. DOI: 10.5923/c.ep.201601.02.
- Kuku, R.O., Adefuye, O.A., Fadipe, O.L., Adebawale, G.I., & Delogan, O.M. (2020). Development of Groundnut Oil Expelling Machine. *Engineering & Technology Research Journal*, 5(2), 93-100. <https://doi.org/10.47545/etrj.2020.5.2.072>
- Kyaw, A., Su Pon, C., & Khin, H. (2019). Design and stress analysis of screw shaft for peanut oil screw press expeller. *International Journal of Progressive Science and Technologies*, 16 (1), 1263.
- Linus, A.A., Mogaji, T.S., & Olabanji, O.M. (2023). A Comprehensive analysis of oil extraction technologies for optimized biodiesel production. *Journal of Energy Research and Reviews*, 15(4), 63-81. <https://doi.org/10.9734/jenrr/2023/v15i4325>
- Maigul, M., Mukhtarbek, K., Amirzhan, K., Bauyrzhan, I., Zhadra, S., Esen, K., Gulmira, Z., Assem, S., Gulnara K. and Anuarbek, S. (2023). Mathematical Modeling of Screw Press Configuration for Processing Safflower Oil. *Journal of applied science*, (13), 3057. <https://doi.org/10.3390/app13053057>
- Moses, D. (2016). Performance evaluation of continuous screw press for extraction soybean oil. *American journal of science and technology*, 1(5), 238-242.
- Muhammad, M.A., & Sohail, I. (2024). Design and analysis of novel microelectromechanical system based microgripper for manipulating microbiological species and micro objects. *Journal of Mechanical Engineering Science*, 238(18), 1–18. <https://doi.org/10.1177/09544062241245545>.
- Naquib, M., & Faisal, M. (2020). Development and performance evaluation of an optimized screw type domestic oil expeller. In: *Proceedings of the 5th NA International Conference on Industrial Engineering and Operations Management*, Detroit, Michigan, USA, 10-14 August.
- Oji, N., Gwarzo, M.A., Mohammed, S.U., Abubakar, I., Agunsoye, K.J., Zakariyah, A., & Adamu, I.E. (2019). Design and Construction of a Small-Scale Sugarcane Juice Extractor. *Asian Research Journal of Agriculture*, 11(4),1-8. <https://doi.org/10.9734/arja/2019/v11i430064>

- Ojo, O.T., Mogaji, T.S., Adeyeri, M.K. Ayodeji, S.P., & Fagbemi, T.N. (2022). Design and finite element analysis of an industrial-based vegetable leaf washing machine. *Journal of engineering and engineering technology*, 16(1), 82 -94. <http://doi.org/10.51459/futajeet.2022.16.1.414>.
- Omojola, A., & Daramy, V.V. K (2023). Application of machine learning technologies in biodiesel production process – A review. *Journal of frontier in energy research*, 10(3), 20 -32.
- Orhorhoro, E.K., Ikpe, A.E., & Tanmuno, R.I. (2016). Performance Analysis of Locally Design Plastic Crushing Machine for Domestic and Industrial Use in Nigeria. *European Journal of Engineering Research and Science*, 1(2), 26-30. <https://doi.org/10.24018/ejeng.2016.1.2.153>
- Oyejide, O.J., Omeche, V.M., Elkanah, S.B., Adeleke, T.B. (2018). Design and construction of a palm kernel oil extraction machine. *Nigerian journal of engineering science research*, 1(1), 22-29.
- Ragul, K.E., Kiruthika, S., & Chandrasekaran, M. (2019). Transesterification of castor oil for biodiesel production: Process optimization and characterization. *Microchemical Journal*, (145), 162-1168. <https://doi.org/10.1016/j.microc.2018.12.039>
- Rajput, R.K. (2007). *Engineering Thermodynamics*, Third Edition, S.I units' version. Laxmi Publications, New Delhi.
- Rattanaphra, D., & Srinophakun, P. (2010). Biodiesel production from crude sunflower oil and crude jatropha oil using immobilized lipase. *Journal of Chemical Engineering*, (43), 104–108. <https://doi.org/10.1252/jcej.09we010>
- Rufus, O.C., Samuel, I.U., Abdulrahim, A.T., Anthony, I., Benjamin, I.C., & Ukwu, N. (2015). Design, modelling and simulation of palm kernel oil extraction machine management approach. *International Journal of Advancements in Research & Technology*, 4(10), 2278-7763.
- Said, M.A.I., Abed, K.A., Gad, M.S., & Abu Hashish, H.M. (2024). Performance and emissions of a diesel engine burning blends of Jatropha and waste cooking oil biodiesel. *Journal of Mechanical Engineering Science*, 238(4), 1157–1169. <https://doi.org/10.1177/09544062231181809>
- Salawu, T.A., Isiaka, M., & Suleiman, L.M. (2015). Development of an oil extraction machine for jatropha curcas seeds. *Journal of Scientific Research & Reports*, 6(4), 313-328. <https://doi.org/10.9734/JSRR/2015/15148>
- Sánchez, N., Sánchez, R., Encinar, J.M., González, J.F., & Martínez, G. (2015). Complete analysis of castor oil methanolysis to obtain biodiesel. *Fuel*, (147), 95-99. <https://doi.org/10.1016/j.fuel.2015.01.062>
- Sarip, M.S.M., Morad, N.A., & Yamashita, Y. (2016). Crude palm oil (CPO) extraction using hot compressed water (HCW). *Sep Purif Technology*, (169), 103–112. <https://doi.org/10.1016/j.seppur.2016.06.001>
- Sujata, B., Biswajit, N., Bidangshri, B., Bipul, D., Pankaj, S., Khemnath, P., & Sanjay, B. (2022). Biodiesel production from mixed oils: A sustainable approach towards industrial biofuel production. *Chemical Engineering Journal Advances*, 10(5), 100284. <https://doi.org/10.1016/j.ceja.2022.100284>
- Teklit, G.A., Mentore, V., Adrian, B., Shiv, P., Eric, v. H., Sami, R. (2021). Emerging technologies for biofuel production: A critical review on recent progress, challenges and perspectives. *Journal of Environmental Management*, (290), 112627. <https://doi.org/10.1016/j.jenvman.2021.112627>
- Vikram, M., & Elliot, L. (2024). Aligning Advances in Biodiesel Technology with the Needs of the Defense Community, (5), 2709–2727. <https://doi.org/10.3390/eng5040142>.
- Wadhah, H.A., Obed, M.A., Ahmed H.A., Hasan, K. (2022). Comparative study of biodiesel production from different waste oil sources for optimum operation conditions and better engine performance. *Journal of Thermal Engineering*, 8(4), 457–465. <https://doi.org/10.18186/thermal.1135266>
- Wunuken, C., Oladele, A., & Sa'ad, A. (2019). Improving jatropha biodiesel yield through the box-behinken process variables optimization method. *International Journal of Engineering Science and Research Technology (IJESRT)*, 8(1), 118-126.
- Yakubu, U.A., Muhammad, S.U., Isiaka, M., Sada, M.A., & Saleh, A. (2020). Development of Castor (Ricinus Commnis) Seeds Shelling Machine. *Nigerian Journal of Engineering*, 27(3), 0794 – 4756.
- Yunus, A.C., & Afshin, J.G. (2015). *A Textbook on Heat and Mass Transfer Fundamentals and Applications*, Fifth Edition; McGraw-Hill Education, New York.
- Ziemiński, K., & Fraç, M. (2012). Methane fermentation process as anaerobic digestion of biomass: Transformations, stages and microorganisms. *African Journal of Biotechnology*, 11(18), 206 – 507. <https://doi.org/10.5897/AJBX11.054>
- Zulqarnain, M.A., Mohd, H.M.Y., Muhammad, H.N., Imtisal, Z., Mariam, A., Farooq, S., Dita, F., & Eduardus, B.N. (2021). A comprehensive review on oil extraction and biodiesel production technologies. *Journal of sustainability*, 13(2), 788. <https://doi.org/10.3390/su13020788>